

Electrocatalytic Activities of Nano-Sized Spinel-Type $\text{Cu}_x\text{Co}_{3-x}\text{O}_4$ ($0 \leq x \leq 1$) for Methanol Oxidation in Alkaline Solutions

R. N. Singh*, T. Sharma, A. Singh, Anindita, D. Mishra

Department of Chemistry, Faculty of Science, Banaras Hindu University, Varanasi – 221005, INDIA

*E-mail: rnsbhu@rediffmail.com

Received: 10 July 2007 / Accepted: 13 August 2007 / Published: 1 October 2007

Nano-sized spinel-type $\text{Cu}_x\text{Co}_{3-x}\text{O}_4$ ($x = 0, 0.3, \text{ and } 1.0$) have been prepared by the hydroxide-carbonate co-precipitation method at 350°C and investigated their electrocatalytic activities towards methanol oxidation in alkaline solutions at 25°C using cyclic voltammetry, chronoamperometry, impedance spectroscopy and anodic Tafel polarization techniques. The reaction indicated a Tafel slope of $\sim 2.303RT/F$ and order w.r. to $[\text{OH}^-]$ and $[\text{CH}_3\text{OH}] \sim 1$ and ~ 0.5 , respectively. The rate of electro-oxidation of methanol was found to increase with increasing substitution of Cu for Co in the oxide matrix. The apparent methanol oxidation current densities found on these oxide anodes at $E = 0.5\text{V}$ versus Hg / HgO in a mixture of 1M KOH and 1M CH_3OH were $\sim 26, \sim 39$ and $\sim 45 \text{ mAcm}^{-2}\text{mg}^{-1}$ for $x = 0, x = 0.3$ and $x = 1.0$, respectively. The oxide electrodes did not show any surface poisoning by methanol oxidation intermediates / products during chronoamperometry experiments. Based on results, a suitable mechanism for the oxidation reaction has been suggested.

Keywords: Nano-sized; Spinel-type; Methanol oxidation; Electro-oxidation; Oxide anodes

1. INTRODUCTION

Direct methanol fuel cell (DMFC) is considered a potential candidate for power generation in electric vehicles [1, 2]. However, one of the major difficulties in commercialization is, perhaps, the high over-potential associated with direct electro-oxidation of methanol [3, 4]. Electrocatalysts especially based on Pt [4-11] and Pt-Ru alloys [4, 12-17] are found to exhibit good activities for electro-oxidation of methanol, but their high costs possibly prohibit them for practical use. Also, these anodes undergo loss in activity with time due to poisoning by the methanol oxidation intermediates [4]. To reduce the cost vis-à-vis to enhance the surface area and hence the electrocatalytic activity, noble metals and alloys have recently been produced in highly dispersed forms. For the purpose,

various supports, such as WO_x [18], graphite [19], multiwalled carbon nanotubes (MWCNTs) [20], polyoxometalate-modified carbon nanotubes [21], and nanowire array [22] were used. Besides these anodes, oxides of V, Fe, Ni, In, Sn, La, and Pb [23], non noble metallic glasses [24] and carbides [25] were also investigated, none of these anodes have shown any measurable activity for methanol oxidation except the carbides. The major problem associated with metallic glasses appears to be of the stability of the electrode during operating conditions [26].

A survey of literature reveals that though complex oxides of transition metals, particularly Co- and Ni- based belonging to spinel or perovskite family have extensively been investigated as anodes for alkaline water electrolysis [27-31], they seem to be little investigated as anode electrocatalysts for methanol oxidation. Only very recently, Raghuvver and Vishwanathan [26], Raghuvver et. al. [32] and Yu et al [33] reported the electrocatalytic activities of $\text{La}_{2-x}\text{Sr}_x\text{CuO}_4$, $\text{La}_{2-x}\text{M}_x\text{Cu}_{1-y}\text{M}'_y\text{O}_4$ (where $\text{M} = \text{Sr, Ca, and Ba}$; $\text{M}' = \text{Sb and Ru}$), and $\text{La}_{1-x}\text{Sr}_x\text{MO}_3$ ($\text{M} = \text{Co or Cu}$), respectively, towards electro-oxidation of methanol in alkaline solutions. The electrocatalytic activities of these oxides determined in terms of current densities at $E = 0.60 \text{ V vs. Hg/HgO}$ were ranged between 0.38 and 18.8 mAcm^{-2} . However, there is lacking of investigation of the methanol oxidation on oxides belonging to spinel family. It is, therefore, desired to carry out a detailed investigation relating to mechanism of methanol oxidation on these oxides in alkaline media, as these oxides are low cost, easily available and have outstanding corrosion stability in alkaline solutions. Also, they can be used as support of precious metal catalysts to enhance the activity for alcohol oxidation at lower metal loadings. In view of this, we have prepared spinel-type $\text{Cu}_x\text{Co}_{3-x}\text{O}_4$ and investigated the mechanism for oxidation of methanol in KOH solutions; details of results obtained are presented in the present paper.

2. EXPERIMENTAL PART

$\text{Cu}_x\text{Co}_{3-x}\text{O}_4$ oxides with $x = 0$, $x = 0.3$ and $x = 1.0$ were prepared following a hydroxide-carbonate co-precipitation method as described elsewhere [28]. In this method, stoichiometric quantities of nitrates of Cu and Co were dissolved in distilled water and to this a saturated Na_2CO_3 solution was added in drop-wise manner with constant stirring at 60°C so as to precipitate metal ions as metal carbonates completely. The precipitate was filtered, washed thoroughly in distilled water, dried at 120°C for 24 h and then decomposed at 350°C for 4h in air to obtain the desired oxide. The formation of oxides has been confirmed by recording X-ray powder diffraction diagrams on an X-ray diffractometer (Rigaku, Japan) using CuK_α as the radiation source ($\lambda = 1.54056 \text{ \AA}$).

The oxide film electrode was obtained by painting a slurry of oxide powder with glycerol onto one side of the pretreated nickel support (geometric surface area: $1.5 \text{ cm} \times 1 \text{ cm}$, Aldrich 99.7% purity) and on subsequent sintering at 340°C for 2h. The procedure followed in the treatment of the nickel support and making an electrical contact to the oxide film were similar to those described elsewhere [28].

A conventional three- electrode single- compartment Pyrex glass cell, involving a pure Pt-foil ($\sim 8\text{cm}^2$) and an Hg/HgO/1M KOH respectively as auxiliary and reference electrodes, was employed for electrochemical investigations. All potential values given in the text correspond to this reference

only. Studies of cyclic voltammetry, impedance and anodic Tafel polarization were carried out using an electrochemical impedance system (Model 273 A, EG & G, PARC, USA) provided with a lock-in-amplifier (Model 5210), a potentiogalvanostat (Model 273A) and a PS/2 (COMPAQ 5500) computer. The softwares used in impedance and Tafel polarization measurements were Power Sine and M 352 Corrosion analysis, respectively.

The electrochemical impedance study of the oxide film electrodes in an alkaline methanol solution has been carried out with an ac voltage amplitude of 10 mV and at a constant dc potential. The frequency range employed was 0.02-10⁵ Hz. The circuit parameters were analysed using the ZSimpWin software.

Cyclic voltammetry of each electrocatalyst has been investigated between 0 and 0.7V versus Hg/HgO in Ar saturated 1M KOH with and without containing methanol at 25⁰C. Before recording the final voltammogram each electrode was cycled for five runs at a scan rate of 50mVs⁻¹. The anodic polarization curves (E versus log j) were recorded using a run program with conditioning time = 200 s, conditioning potential = 0.35 V, initial delay = pass, scan rate = 0.2 mVs⁻¹, initial potential = 0.35 V and IR interruption = 10 s.

The chronoamperometric experiment on each oxide electrocatalyst was carried out in 1 M KOH (Merck, GR) + 1 M CH₃OH (Glaxo) at a fixed potential (E = 0.40 Vvs. Hg/HgO) at 25⁰C.

All the electrochemical experiments have been performed in Ar deoxygenated electrolytes at 25⁰C.

3. RESULTS AND DISCUSSION

3.1. X-ray diffraction (XRD)

Fig.1 represents the XRD patterns of oxides recorded between 2θ = 0 and 100⁰. This figure shows that the carbonate method produces almost pure and crystalline spinel phase. The crystallite followed the face centered cubic crystal geometry. Values of the unit cell dimension (a) were found to be 8.04, 8.095 and 8.055 Å respectively for the oxide with x = 0, 0.3 and 1.0. However, a-value observed for Co₃O₄ is lower than its corresponding literature value (a = 8.084 Å, JCPDS ASTM file No. 9-418) while for CuCo₂O₄ is higher than its corresponding value reported in literature (a = 8.039 Å, JCPDS ASTM file No. 1-1155). Thus, introduction of Cu increases the a-value, the effect, however, being considerable with x = 0.3. This increase can be attributed to the higher radii of Cu²⁺ in the coordination number 4 (0.57 Å) and 6 (0.73Å) compared to that of Co²⁺ (coordination No.4: 0.56 Å & coordination No.6: 0.65 Å). The crystallite size (S) was estimated using the Scherrer's formula [34] and values were ~17, ~16, and ~11 nm for the oxide with x = 0, 0.3 and 1.0, respectively.

3.2. Cyclic voltammetry

Cyclic voltammograms for Cu_xCo_{3-x}O₄ (x = 0, 0.3 & 1.0) electrodes in 1 M KOH were determined in the potential range of 0 to 0.70 V versus Hg/HgO and at a potential scan rate of 10 mVs⁻¹ at 25⁰C. These oxides exhibited the usual single couple of anodic and cathodic redox peaks at E_{pa} =

520 ± 18 and $E_{pc} = 282 \pm 7$ mV, respectively, revealing a pseudo-capacitance due to Co(IV) / Co(III) surface redox couple [28-29]. A typical voltammogram obtained in the case of Co_3O_4 electrode, as an example, is shown in Fig. 2. Cu substitution slightly decreases (~ 10 mV) the formal redox potential [$E^0 = (E_{pa} + E_{pc}) / 2$] of the couple, Co (IV) / Co(III).

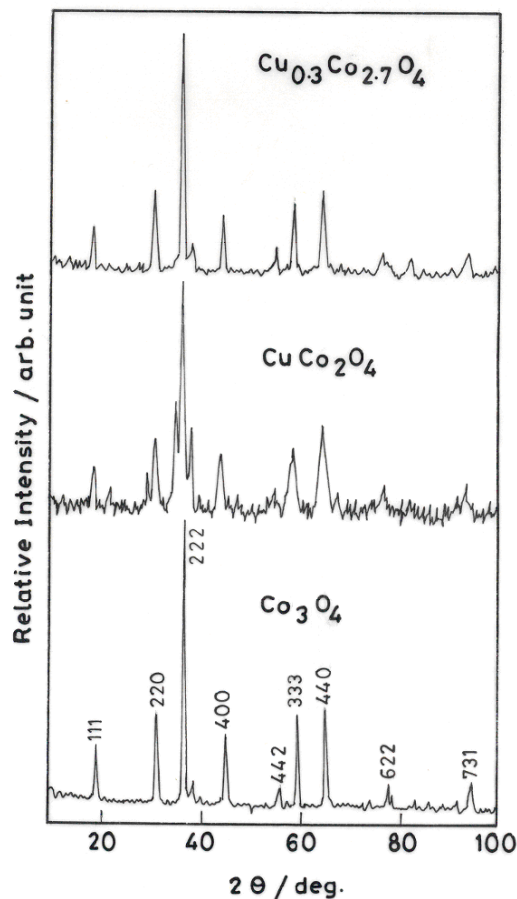


Figure 1. XRD powder patterns for $\text{Cu}_x\text{Co}_{3-x}\text{O}_4$ with $x = 0$, $x = 0.3$ and $x = 1.0$ sintered at 350°C for 5h.

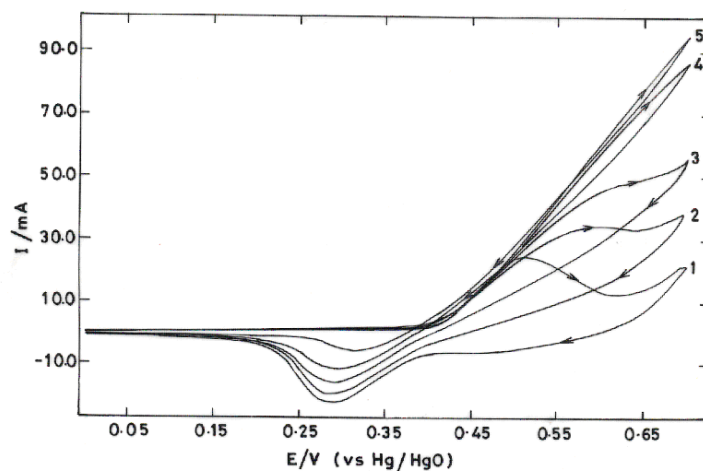


Figure 2. Typical cyclic voltammograms for Co_3O_4 electrode (geometrical area = 0.45 cm^2) in the potential region, 0-0.7 V (vs. Hg/HgO), at 10 mVs^{-1} in 1 M KOH containing (1) 0.0 M, (2) 0.1M, (3) 0.2 M, (4) 0.5 M and (5) 1.0 M CH_3OH (25°C).

Volammograms for the electrodes were also recorded in 1M KOH containing varying no. of mols of methanol and curves so obtained in each case were very similar. Voltammograms obtained in the case of Co_3O_4 electrode are represented in Fig.2. This figure shows that in the presence of 0.1 M CH_3OH in 1 M KOH solution, the anodic peak current enlarges while its corresponding cathodic peak diminishes, indicating thereby a strong interaction between the higher valence Co(IV) species and methanol. Subsequent increases of methanol concentrations tend to highly increase and merge the anodic peak into the anodic wall of the voltammogram's window. Further, the cathodic peak current for the electro-reduction of Co(IV) to Co(III) decreases with increasing the methanol concentration while it increases with increasing the potential scan rate (Fig. 3)

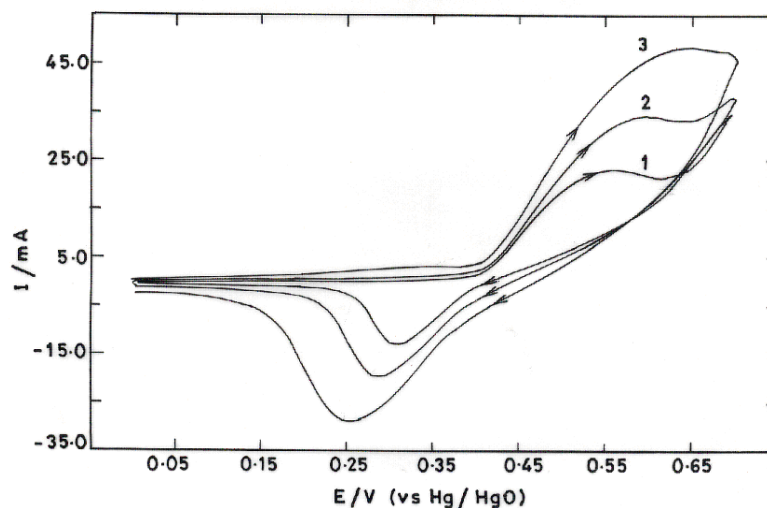


Figure 3. Typical cyclic voltammograms for Co_3O_4 electrode (geometrical area = 0.45 cm^2) in the potential region, 0-0.7 V (vs. Hg/HgO), at varying scan rates in a mixture of 1 M KOH and 0.1M CH_3OH (25°C). Scan rates: 5 (1), 10 (2) and 20 (3) mVs^{-1}

Results of the cyclic voltammetry study indicate that methanol molecules interact with the higher valence Co(IV) species and reduce them into Co(III) species in a, rather, slow step as compared to their transformation into Co(IV) species through electrochemical oxidation under the anodic condition. At higher scan rates methanol is not capable of reducing all the available higher valence Co(IV) species in the oxide surface layer and, therefore, the remaining Co(IV) species get reduced under the cathodic condition producing the corresponding cathodic peak. The higher the scan rate the greater would be the cathodic peak current. Similar results were also obtained in the case of the electrolytic oxidation of methanol on a cobalt hydroxide modified glassy carbon electrode in alkaline medium [2]. Furthermore, at higher methanol concentrations and under anodic condition, the oxidation current observed during the reverse scan intersects the oxidation current observed during the forward scan and gets slightly shifted towards the lower potential region. This can be attributed to electrochemical oxidation of some oxidation intermediates at relatively lower potentials.

The comparison of voltammogram for methanol oxidation on a particular oxide electrode with that of the same electrode obtained in purely 1 M KOH shows that the onset potentials for methanol oxidation ($E = 0.350\text{-}0.366 \text{ V vs Hg / HgO}$) is more or less the same as the onset potential for the

Co(III) to Co(IV) oxidation (0.368-0.400 V vs Hg / HgO). Thus, the oxidation of methanol takes place in the potential region associated with formation of Co (IV).

3.3. Chronoamperometry

Chronoamperograms of electrodes were also recorded at $E = 400\text{mV}$ in 1M KOH containing 1M CH_3OH for nearly one hour and curves so produced are shown in Fig.4. The feature of curves shown in Fig 4 clearly demonstrates that there is little deactivation of the electrode during the oxidation of CH_3OH in 1M KOH. Also, the electrode with $x = 0.3$ has the greatest catalytic activity for oxidation of CH_3OH while the electrode with $x = 0$ has the least catalytic activity.

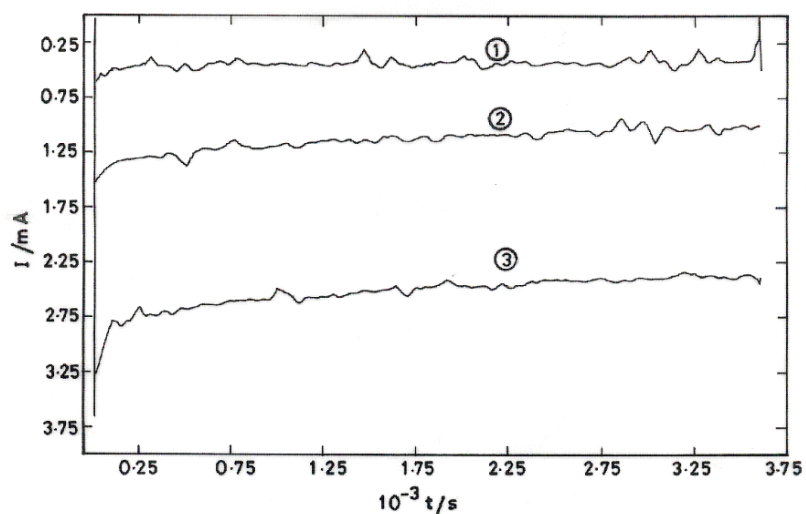


Figure 4. Chronoamperograms of $\text{Cu}_x\text{Co}_{3-x}\text{O}_4$ electrodes at $E = 0.4\text{ V}$ vs. Hg/HgO in a mixture of 1M KOH and 1M CH_3OH (25°C). $x = 0$ (1), $x = 1.0$ (2) and $x = 0.3$ (3).

To obtain some vital clue to the mechanism of methanol electro-oxidation, cyclic voltammetry and chronoamperometry studies of HCHO and HCOOK were also carried out at the base oxide (Co_3O_4) electrode in 1 M KOH and the results, so obtained, are shown in Fig. 5 & 6. Both HCHO and HCOOK are considered as the possible intermediate products of methanol oxidation. Fig 5 demonstrates that the onset potential for oxidation of HCHO is nearly 240 mV more negative than that for methanol oxidation. However, the observed oxidation current in the case of CH_3OH , which is considerably low compared to HCHO at low potentials, becomes greater than that found with HCHO at the higher potential, under similar experimental conditions. The onset potentials for oxidation of CH_3OH and HCOO^- were very close to each other. Further, Fig.6 demonstrates that the oxide anode does not suffer any appreciable deactivation due to poisoning by intermediates/products of oxidation of $\text{CH}_3\text{OH}/\text{HCOO}^-$. However, an appreciable deactivation of the electrode takes place in the case of oxidation of HCHO. These results indicate that the oxidation of methanol possibly involve intermediates which possess little poisoning effect on the electrode surface in alkaline medium. Hence, based on the deactivation of the electrode in the case of oxidation of HCHO, HCHO species cannot be considered as intermediates in the case of electro-oxidation of methanol.

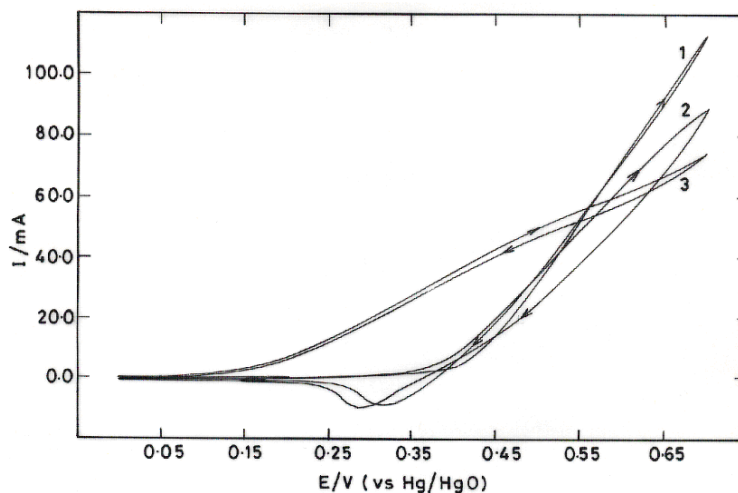


Figure 5. Cyclic voltammograms for Co_3O_4 electrode (geometrical area = 0.4 cm^2) at 10 mVs^{-1} in the potential region, 0- 0.7 V vs Hg/ HgO, in binary mixtures of (1) 1M KOH and 1M CH_3OH , (2) 1M KOH and 1M HCOOK and (3) 1M KOH and 1M HCHO (25°C).

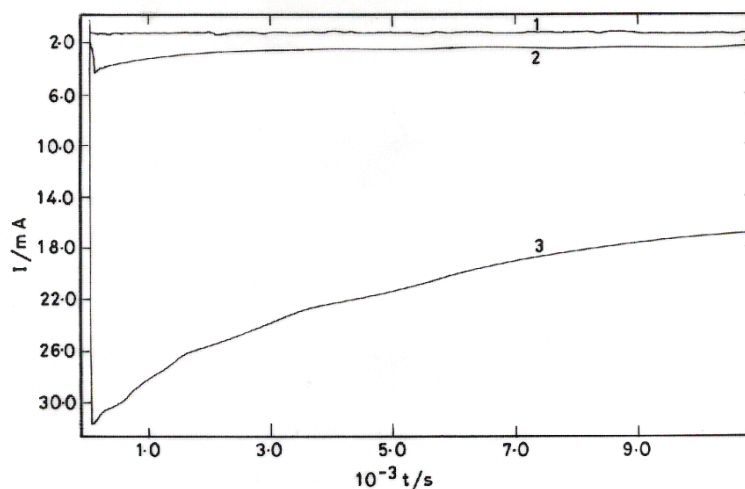


Figure 6. Chronoamperograms for Co_3O_4 electrode (geometrical area = 0.4 cm^2) at $E = 0.4 \text{ V}$ vs Hg/HgO in binary mixtures of (1) 1M KOH and 1M CH_3OH , (2) 1M KOH and 1M HCOOK and (3) 1M KOH and 1M HCHO (25°C).

After the chronoamperometry test was over, a saturated BaCl_2 solution was added into the cell solution which showed the presence of carbonate as one of the products of the oxidation reaction [35]. Thus, this test demonstrates that methanol is finally oxidized to CO_2 .

3.4. Roughness Factor

The oxide roughness factor/electrochemically active area of electrocatalyst was estimated by measuring the charging current density as a function of scan rate in 1M KOH at 25°C , details of which can be found elsewhere [27, 34]. For the purpose, cyclic voltammograms in a small potential region, 0 – 0.1V vs Hg/HgO, wherein the charge-transfer reactions were almost negligible, were recorded at

varying scan-rates (10 – 250mV/s). The value of the double layer capacitance was calculated by measuring the slope of the linear j_{cap} versus scan rate plot at $E = 0.05$ V vs. Hg/HgO. Cyclic voltammograms for the $\text{Cu}_{0.3}\text{Co}_{2.7}\text{O}_4$ electrode, as a typical example, and the j_{cap} vs scan rate plot for all the three electrodes are shown in Figs. 7 and 8, respectively. Curves shown in Fig. 7 are linear up to a scan rate of ~ 140 mVs^{-1} in the case of oxide electrodes with $x = 0$ and 0.3 while with $x = 1$, it looks to be linear in the whole region of the applied scan rate (i.e., 250 mVs^{-1}). The observed deviation from

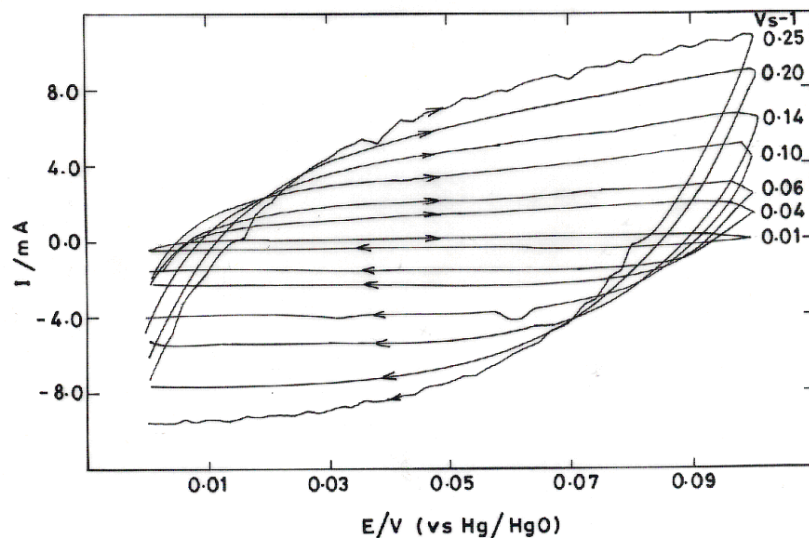


Figure 7. Typical cyclic voltammograms for $\text{Cu}_{0.3}\text{Co}_{2.7}\text{O}_4$ electrode (geometrical area = 0.45 cm^2) in the potential region, $0 - 0.1$ V vs. Hg/HgO, in 1M KOH and at varying scan rates (25°C).

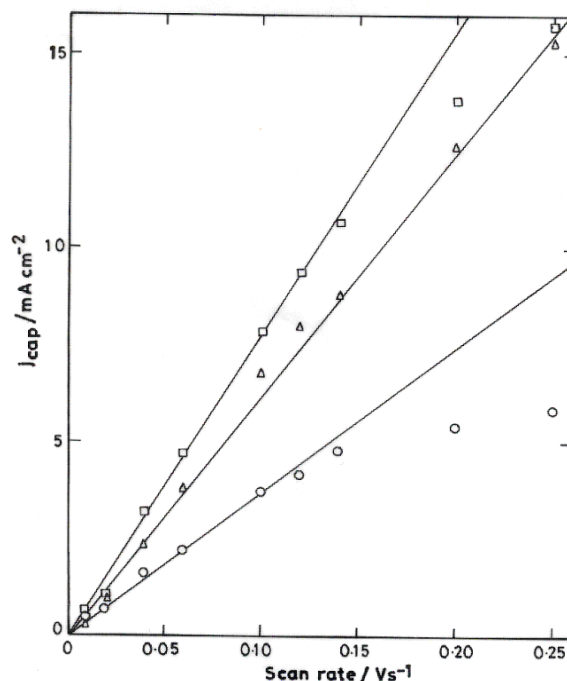


Figure 8. Plots of j_{cap} versus scan rate for $\text{Cu}_x\text{Co}_{3-x}\text{O}_4$ electrodes at $E = 0.05$ V in the potential region, $0 - 0.1$ V vs. Hg/HgO in 1M KOH (25°C). Curves: o, $x = 0$; □, $x = 0.3$ and Δ, $x = 1.0$.

linearity might be due to exclusion of some inner surface area at high scan rates [36]. The C_{dl} value determined for the oxide electrodes were 0.0236, 0.109 and 0.068 $F\text{cm}^{-2}$ for Co_3O_4 , $\text{Cu}_{0.3}\text{Co}_{2.7}\text{O}_4$ and CuCo_2O_4 , respectively. The corresponding values for the roughness factor (R_F) based on the double layer capacitance of smooth oxide surface ($60 \mu\text{F cm}^{-2}$ [37]) were found to be 390, 1820 and 1130, respectively. Assuming the total mass of deposited oxide as active, the corresponding values of the oxide roughness factor per mg of the oxide loading ($R_f = R_F / \text{oxide mass}$) were ~ 200 , ~ 393 and ~ 474 . Thus, results show that replacement of Co by Cu in Co_3O_4 increases the oxide roughness significantly.

3.6. Electrochemical impedance spectroscopy (EIS)

The EIS study of oxide electrodes was carried out to investigate the reaction process and kinetics of methanol oxidation in different Ar-deoxygenated aqueous alkaline methanol solutions. The study was conducted both, in the presence and absence of methanol. Effects of methanol and OH^- concentrations as well as of the applied potential were also examined on the impedance behavior of the oxide electrodes. Before recording each EI spectrum at a pre-selected dc potential, the working electrode was first kept at this potential for 300 seconds to equilibrate. Features of EIS spectra obtained on each oxide anode under similar experimental conditions were very similar.

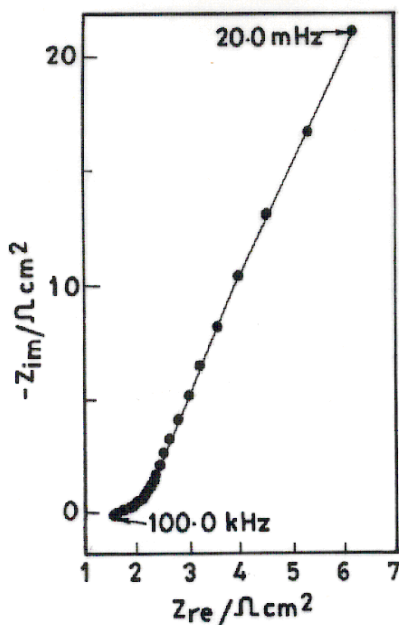


Figure 9. Typical Nyquist plot for Co_3O_4 electrode at $E = 0.45 \text{ V}$ in 1M KOH at 25°C .

It is observed that, in the absence of CH_3OH , the Nyquist plots for all the three oxide electrodes do not exhibit any visible semicircle at high frequencies while they indicate a capacitive-type behaviour at the low frequencies (\sim less than 6 Hz). A typical Nyquist plot for the base electrode (Co_3O_4) is shown in Fig.9. However, in the presence of methanol, each Nyquist curve indicates two arcs, a small arc at high frequencies and a larger one showing the formation of a semicircle at the low frequencies. The diameter of the semicircle, formed at low frequencies is found to be greatly

influenced with the change of the electrolyte concentration (CH_3OH and KOH). The three representative Nyquist curves in the case of the base oxide in presence of methanol are given in Fig.10. The diameter of the semicircle at low frequencies was also decreased with the applied potential across the oxide-solution interface as is quite evident from the representative curves displayed in Fig.11. It was noted that the high frequency arc changes little by the change in methanol, KOH or potential. Thus, the results indicate that the low frequency arc corresponds mainly to the charge transfer methanol oxidation reaction.

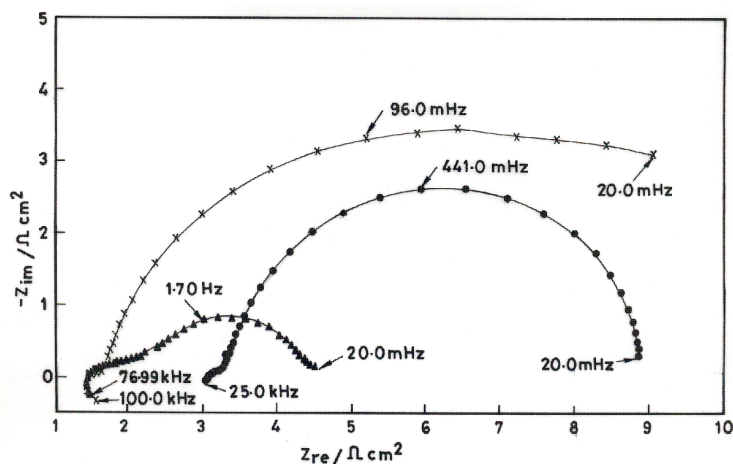


Figure 10. Typical Nyquist plots for Co_3O_4 electrode at $E = 0.45$ V in binary mixtures of (x) 1M KOH and 0.1 M CH_3OH , (●) 0.5M KOH and 1 M CH_3OH and (▲) 1M KOH and 1 M CH_3OH (25°C).

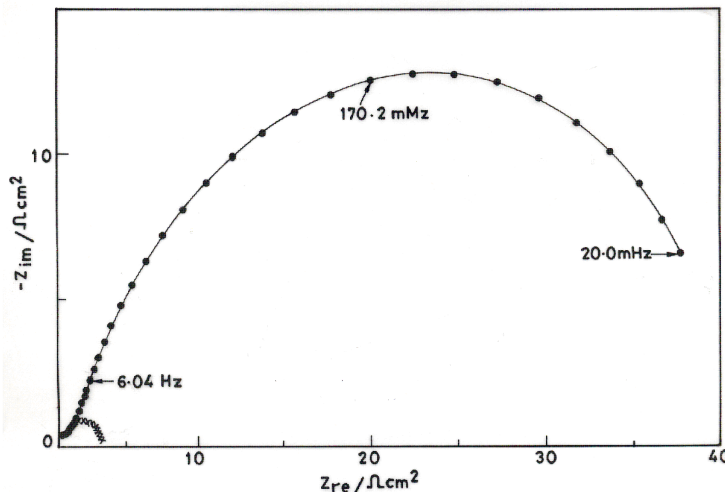


Figure 11. Typical Nyquist plots for Co_3O_4 electrode (geometrical area = 0.45 cm^2) at two potentials in a mixture of 1M KOH and 1M CH_3OH (25°C); (●) $E = 0.40$ & (x) : 0.45 V vs. Hg/HgO .

The experimental data were analysed by the equivalent circuit with circuit description code (CDC), $\text{LR}_s(\text{R}_1\text{Q}_1)(\text{R}_2\text{C}_2)$. Symbols used in CDC: R_s , R_1 , R_2 , Q_1 and C_2 represent solution resistance, film resistance, charge transfer resistance for methanol oxidation, constant phase element and capacitance, respectively. Table1 shows the value of the equivalent circuit element obtained by fitting the experimental results. The goodness of the fit can be judged by the comparison of simulated and experimentally found EIS spectra as shown in Fig. 12.

Table 1. Values of the equivalent circuit parameters for $\text{Co}_{3-x}\text{Cu}_x\text{O}_4$ electrodes in a binary mixture of methanol and KOH at 25°C.

x	Loading mg/cm^2	Electrolyte	E V	L x 10^7 Hcm^2	R_s Ωcm^2	R_1 Ωcm^2	Q_1 $\text{Fs}^{n-1}/\text{cm}^2$	n_1	R_2 Ωcm^2	C_2 Fcm^{-2}
0	3.08	1M KOH + 0.1MCH ₃ OH	0.45	3.02	1.72	0.93	0.149	0.55	10.6	0.108
0	3.08	1M KOH + 1M CH ₃ OH	0.45	5.72	1.41	1.43	0.055	0.45	1.87	0.049
0	3.30	1M KOH + 1MCH ₃ OH	0.40	7.22	1.73	3.39	0.025	0.52	46.0	0.006
0	3.30	1M KOH + 1MCH ₃ OH	0.50	0.11	1.65	1.36	0.038	0.53	0.88	0.011
0	3.30	0.5M KOH +1MCH ₃ OH	0.45	1.32	3.02	0.36	0.029	0.70	5.82	0.048
0.3	3.30	1M KOH + 0.1MCH ₃ OH	0.45	-----	2.89	1.90	0.224	0.58	20.71	0.069
0.3	3.30	1M KOH + 1M CH ₃ OH	0.45	3.43	1.89	0.92	0.104	0.48	1.40	0.044
1.0	2.34	1M KOH + 0.1MCH ₃ OH	0.45	7.99	0.90	0.76	0.251	0.57	14.29	0.060
1.0	2.34	1M KOH + 1MCH ₃ OH	0.45	7.52	1.07	1.06	0.095	0.48	1.09	0.040

Table 1 shows that R_2 -value decreases and hence the rate for electro-oxidation of methanol increases with the increase in potential and also with increase in KOH or methanol concentration in the electrolyte. This would be more clear in the study of electrode kinetics of the reaction.

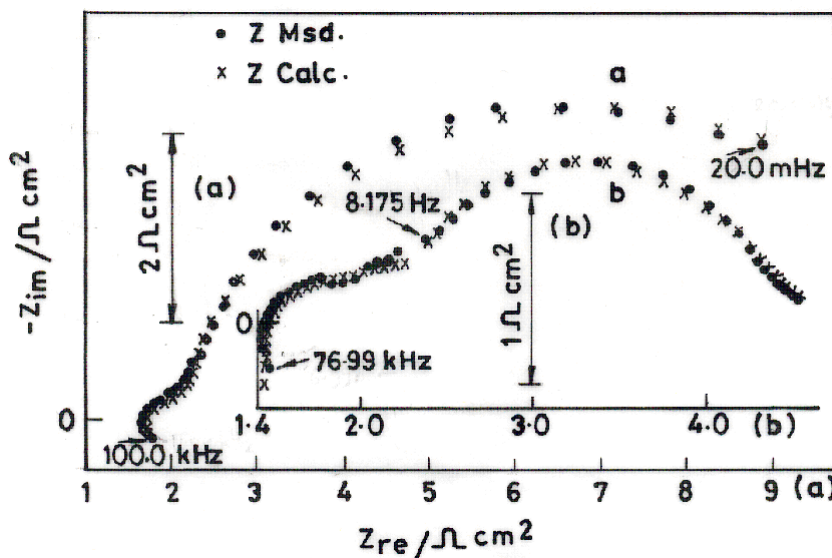


Figure 12. Typical Nyquist plots (measurement + simulation) for Co_3O_4 electrode (geometrical area = 0.45 cm^2) at $E = 0.45 \text{ V}$ vs. Hg/HgO in binary mixtures of (a) 1M KOH and 0.1 M CH_3OH and (b) 1 M KOH and 1M CH_3OH (from Fig. 10).

3.7. Electrode kinetic study

To investigate the mechanism of electrochemical oxidation of methanol, the IR-compensated E versus $\log j$ curves have been recorded at a low scan rate, 0.2mVs^{-1} , on $\text{Cu}_x\text{Co}_{3-x}\text{O}_4$ electrodes in different KOH and methanol concentrations at 25°C . To obtain the reaction order w. r. to OH^- concentration (p_{OH}), E versus $\log j$ curves for each oxide electrode were determined at varying KOH concentrations maintaining the methanol concentration and the ionic strength of the medium constant ($\mu = 2$) using KNO_3 as an inert salt. A set of four representative E versus $\log j$ curves in the case of Co_3O_4 electrode is given in Fig. 13. The order was determined from the slope of straight lines, $\log j$ versus $\log [\text{KOH}]$, constructed in each case at a constant potential and a constant methanol concentration (2 M) at 25°C . Two representative $\log j$ versus $\log [\text{KOH}]$ plots, one on the base oxide ($x = 0$) at $E = 0.43\text{ V vs. Hg/HgO}$ and $[\text{CH}_3\text{OH}] = 2\text{M}$ and the other on the oxide with $x = 0.3$ at $E = 0.44\text{ V vs. Hg/HgO}$ and $[\text{CH}_3\text{OH}] = 2\text{M}$, are shown in Fig.14. Similarly, the order with respect to the methanol concentration (p_{Me}) was determined by constructing plots, $\log j$ versus $\log [\text{CH}_3\text{OH}]$, at a constant potential and a constant OH^- concentration and measuring the slope of the resulting straight lines. A typical $\log j$ versus $\log [\text{CH}_3\text{OH}]$ plot for the methanol electro-oxidation reaction at $E = 0.41\text{V vs. Hg/HgO}$ and $[\text{KOH}] = 1\text{M}$ is also shown in Fig.14. The order of reaction with respect to methanol and OH^- were found to be respectively 0.5 and 1.

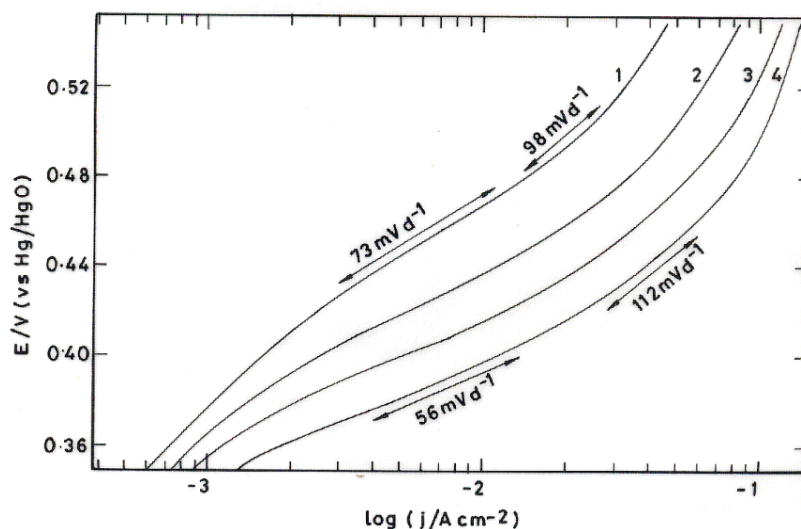


Figure 13. Typical Tafel plots for electro-oxidation of $2\text{M CH}_3\text{OH}$ at Co_3O_4 electrode at varying concentrations of KOH ($\mu = 2\text{M}$) and at 25°C . $[\text{KOH}]$: 0.5 (1), 1 (2), 1.5 (3) and 2 (4) M.

It has been observed that the nature of E versus $\log j$ curves does not change practically by replacement of Co by Cu in the Co_3O_4 matrix. The initial Tafel slope for the reaction is found to be $\sim 60\text{ mVd}^{-1}$ for each oxide electrode. This value of the slope remains almost constant during the variation of concentration of KOH (Fig.12) or alcohol in the electrolyte. Thus, the results suggest that the electro-oxidation of CH_3OH in alkaline solution on $\text{Cu}_x\text{Co}_{3-x}\text{O}_4$ follows similar mechanistic paths. Values of the electrocatalytic activities determined for the three oxide electrodes in a mixture of 1M KOH and $1\text{M CH}_3\text{OH}$ at two different potentials (0.45 and 0.5 V) and of the electrode kinetic

parameters are given in Table 2. Values of j_a shown in Table 2 have not been corrected for the background currents (i.e. current produced in similar experiments carried out in 1M KOH without containing methanol), because the values of the latter were not considerable in the potential region employed for the study. For instance, values of the observed background current in 1 M KOH at 25°C with Co_3O_4 and $\text{Cu}_{0.3}\text{CoO}_4$ at $E = 0.45$ and $E = 0.50$ V vs Hg / HgO were 0.93 and 0.60 and 0.55 and 0.79 mA cm^{-2} , respectively.

Table 2: Electrode kinetic parameters for electro-oxidation of methanol at $\text{Co}_{3-x}\text{Cu}_x\text{O}_4$ anodes in 1M KOH + 1M CH_3OH at 25°C.

x	l (mg/cm^2)	Tafel slope (mVd^{-1})		R_f	Order (p)		j at E (mV)					
		b_1	b_2		p_{me}	p_{OH}	450			500		
							j_a (mA cm^{-2})	j_a (mA cm^{-2} mg^{-1})	$j_t \times 10^2$ (mA cm^{-2})	j_a (mA cm^{-2})	j_a (mA cm^{-2} mg^{-1})	$j_t \times 10^2$ (mA cm^{-2})
0.0	3.1	54	111	200	0.5	1.5	26.93	8.69	4.34	80.27	25.89	12.95
0.3	3.3	55	111	393	0.5	1.2	65.00	19.70	5.01	129.50	39.24	9.98
1.0	2.2	50	108	474	0.5	1.2	58.93	26.79	5.65	99.02	45.01	9.50

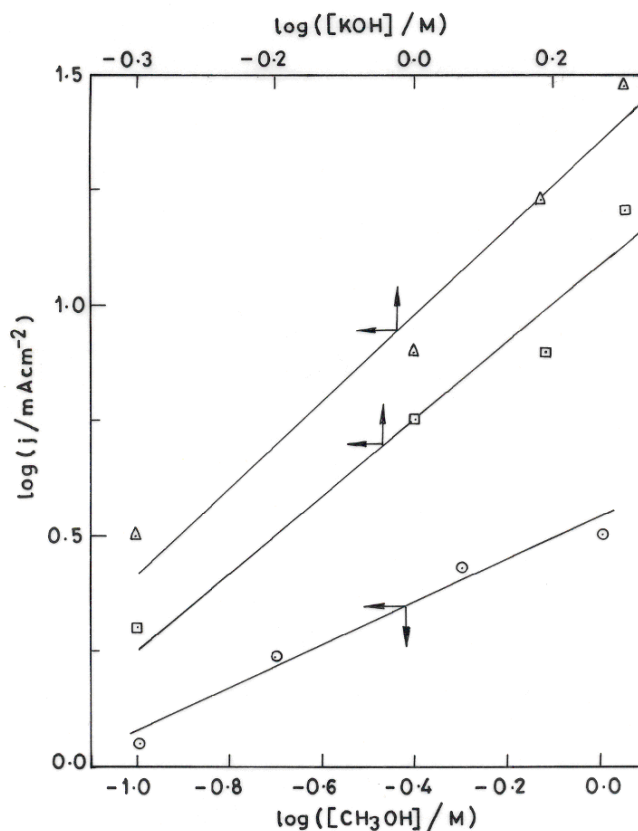


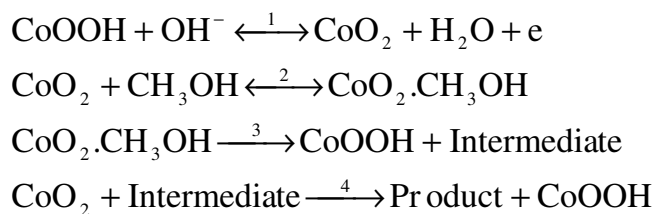
Figure 14. Representative $\log j$ versus $\log [\text{KOH}]$ (or $\log [\text{CH}_3\text{OH}]$) plots for electro-oxidation of 2M CH_3OH at $\text{Cu}_x\text{Co}_{3-x}\text{O}_4$ electrodes at a constant potential (vs. Hg/HgO); $\mu = 2\text{M}$, Δ : $x = 0$ & $E = 0.43$ V, \square : $x = 0.3$ & $E = 0.44$ V and \circ : $x = 0$ & $E = 0.41$ V.

Fig.12 and Table 2 show that Cu addition improves the apparent electrocatalytic activity of methanol oxidation. However, the true electrocatalytic activity of the oxide electrode seems to remain practically unchanged with Cu substitution. Thus, introduction of Cu for Co in the spinel matrix improves geometrical properties but electronic properties of the material do not change practically.

Values of the Tafel slope and the reaction order observed for oxidation of methanol on $\text{Cu}_x\text{Co}_{3-x}\text{O}_4$ are similar to those reported on the (100) Pt surface [38]. A fractional (one half) order kinetics w.r. to methanol concentration has repeatedly been reported in literature [39-40] Yu et al. [6] found $b = 110 \text{ mVd}^{-1}$ on Pt in 0.5M NaOH. However, Tripkovic et al. [5] observed $b = 120 \text{ mVd}^{-1}$ and $p_{\text{me}} = 0.5$ and $p_{\text{OH}} = 0.5$ on (111) and (110) Pt surfaces.

3.8. Mechanism

Results have shown that the electrocatalytic oxidation of methanol seems to be mediated by the $\text{CoO}_2 / \text{CoOOH}$ redox couple. It is believed that the methanol oxidation /dehydrogenation is catalyzed by the $\text{CoO}_2 / \text{CoOOH}$ redox couple. Results of the electrode kinetic study suggest that the alkaline electro-oxidation of methanol on the $\text{Cu}_x\text{Co}_{3-x}\text{O}_4$ surface proceeds through the following mechanistic path:



The above mechanism is similar to that given by Jafarian et al. [2] for the methanol oxidation on cobalt. Considering reaction (3) as the rate determining step (rds) and the total surface coverage by adsorbed methanol under Langmuir adsorption condition, the overall current density expression for the methanol electro-oxidation can be given as,

$$j = nFk_3\theta = nFk_3K_1K_2C_{\text{OH}^-}C_{\text{Me}} \exp(\text{FE}/\text{RT}) \dots \dots \dots (5)$$

where θ is the surface coverage by adsorbed methanol molecules and can be obtained by considering reactions (1) and (2) under quasi-equilibrium conditions. K_1 and K_2 are the equilibrium constants for reactions (1) and (2), respectively. Other symbols involved in the rate equation (5) have their usual meaning.

Eq.5 gives $b \cong 60 \text{ mVd}^{-1}$ and $p_{\text{Me}} = 1$ and $p_{\text{OH}} = 1$. Similar values of the electrode kinetic parameters, namely the Tafel slope and the reaction order with respect to OH^- ion concentration were also found for the methanol oxidation reaction on $\text{Cu}_x\text{Co}_{3-x}\text{O}_4$ at low potentials. The observed fractional reaction order with respect to methanol concentration ($p_{\text{Me}} = 0.5$) indicates that the magnitude of θ is considerable and influences the heats of adsorption and hence the free energies of activation of species to be adsorbed.

4. CONCLUSIONS

The study shows that $\text{Cu}_x\text{CO}_{3-x}\text{O}_4$ with $x = 0, 0.3$ and 1.0 are quite active materials for the methanol electro-oxidation. Cu substitution increases the apparent electrocatalytic of the oxide. The tolerance of the oxide electrodes towards poison by the methanol oxidation intermediates has been excellent. The HCHO oxidation onset potential is found to be nearly ~ 240 mV lower than that of the methanol / HCOO^- oxidation onset potential.

ACKNOWLEDGEMENTS

The work is supported by the Council of Scientific and Industrial Research (CSIR) and the Department of Science and Technology (DST), New Delhi, India through the research projects (Project nos. 01(2033)/06/EMR.II & SR/S1/PC-41).

References

1. X. Ren, P. Zelenay, S. Thomas, J. Davey, S. Gottesfeld, *J. Power Sources* 86 (2000) 111.
2. M. Jafarian, M.G. Mahjani, H. Heli, F. Gobal, H. Khajehsharifi, M.H. Hamed, *Electrochim. Acta* 48 (2003) 3423.
3. G.T. Burstein, C.J. Barnett, A.R. Kucernak, K.R. Williams, *Catal. Today* 38 (1997) 425.
4. R. Parson, T. J. Vandernoot, *J. Electroanalytical. Chem.* 257 (1988) 9.
5. A.V. Tripkovic, K.D. Popovic, J.D. Momcilovic, D.M. Drazic, *Electrochim. Acta* 44 (1998) 1135.
6. E.H. Yu, K. Scott, R.W. Reeve, *J. Electroanal. Chem.* 547 (2003) 17.
7. F. Seland, D.A. Harrington, R. Tunold, *Electrochim. Acta* 52 (2006) 773.
8. T.D. Jarvi, E.M. Stuve, in: J. Lipkowski, P.N. Ross (Eds.), *Electrocatalysis*, Wiley-VCH, New York, 1998, p.75.
9. S. Wasmus, A. Kiiiver, *J. Electroanal. Chem.* 461 (1999) 14.
10. J. Kua, W.A. Goddard, *J. Am. Chem. Soc.* 121 (1999) 10928.
11. T. Iwasita, *Electrochim. Acta* 47 (2002) 3663.
12. S. Tanaka, M. Umeda, H. Ojima, Y. Usui, O. Kimura, I. Uchida, *J. Power Sources* 152 (2005) 34.
13. J. Jiang, A. Kucernak, *J. Electroanal. Chem.* 543 (2003) 187.
14. J.B. Goodenough, A. Hammet, B.J. Kennedy, R. Manohara, S.A. Weeks, *J. Electroanal. Chem.* 240 (1988) 133.
15. W. Sugimoto, T. Saida, Y. Takasu, *Electrochem. Communication* 8 (2006) 411.
16. C. Roth, N. Marty, F. Hahn, J.M. Liger, C. Lamy, H. Fuess, *J. Electrochem. Soc.* 144 (2002) E433.
17. Y. Takasu, W. Sugimoto, Y. Murakami, *Catal. Surve. Asia* 7 (2003) 21.
18. K.-W. Park, K.-S. Ahn, Y.-C. Nah, J.-H. Choi, Y.-E. Sung, *J. Phys. Chem.* 107 (2003) 4352.
19. P.C. Biswas, Y. Nodasaka, M. Enyo, *J. Appl. Electrochem.* 26 (1996) 30.
20. J. Prabhuram, T.S. Zhao, Z.X. Liang, R. Chen, *Electrochim. Acta* 52 (2007) 2649.
21. D. Pan, J. Chen, W. Tao, L. Nie, S. Yao, *Langmuir* 22 (2006) 5872.
22. G.-Yu Zhao, C.-L. Xu, D.-J. Guo, H. Li, H.-L. Li, *J. Power Sources* 162 (2006) 492.
23. T. Ohmore, K. Nodasaka, M. Enyo, *J. Electroanal. Chem.* 281 (1990) 331.
24. K. Machida, M. Enyo, *Bull. Chem. Soc. Jpn.* 58 (1985) 2043.
25. K. Machida, M. Enyo, *J. Electrochem. Soc.* 137 (1990) 871.
26. V. Raghuvier, B. Viswanathan, *Fuel* 81 (2002) 2191.
27. R. N. Singh, J. -F. Koenig, G. Poillerat and P. Chartier, *J. Electrochem. Soc.* 137 (1990) 1408.
28. B. Lal, N. K. Singh, S. Samuel and R. N. Singh, *J. New Mater. Electrochem. Systems* 2 (1999) 59.

29. R. N. Singh, J. P. Pandey, N. K. Singh, B. Lal, P. Chartier and J. -F. Koenig, *Electrochim. Acta* 45 (2000) 1911.
30. S. K. Tiwari, P. Chartier and R. N. Singh, *J. Electrochem. Soc.* 142 (1995) 148.
31. S. K. Tiwari, S. P. Singh and R. N. Singh, *J. Electrochem. Soc.* 143 (1996) 1505.
32. V. Raghuvver, K.R. Thampi, N. Xanthopoulos, H.J. Mathieu, B. Viswanathan; *Solid State Ionics* 140 (2001) 263.
33. H.-C. Yu, K.-Z. Fung, T.-C. Guo, W.-L. Chang; *Electrochim. Acta* 50 (2004) 811.
34. B. Marsan, N. Fradette and G. Beaudoin, *J. Electrochem. Soc.* 137 (1992)1889; N. Fradette, B. Marsan, *J. Electrochem. Soc.* 139 (1992) 1889.
35. A. I. Vogel, A Text-Book of Quantitative Inorganic Analysis, ELBS Press, Longman Group Ltd. New York (1978) p309.
36. R. Boggio, A. Carugati and S. Trasatti, *J. App. Electrochem.* 17 (1987) 828.
37. S. Levine and A. L. Smith, *Discuss. Faraday Soc.* 52 (1971) 290.
38. A. V. Tripkovic, K. Dj.Popovic, J.D. Momcilovic, D. M. Drazic, *J. Electroanal. Chem.* 448 (1998) 173.
39. M.A.A. Rahim, R.M.A. Hameed, M.W. Khalil; *J. Power Sources* 134 (2004) 160.
40. B. Beden, F. Kadirgan, C. Lamy, J. M. Leger, *J. Electroanal. Chem.* 142 (1982) 171.